

Supporting Information

Autocatalytic Photodegradation of $[\text{Ru}(\text{II})(2,2'\text{-bipyridine})_2\text{DAD}]^+$ (**DADH** = 1,2-dihydroxyanthracene-9,10-dione) by Hydrogen Peroxide under Acidic Aqueous Conditions

Lingli Zeng, Dumitru Sirbu, Nikolai Tkachenko and Andrew C. Benniston

Table of Contents

Table S1. ^1H NMR chemical shifts (ppm) for Δ - RDAD in CD_3CN at R.T.	2
Figure S1. Labelled HSQC spectrum for Δ - RDAD in CD_3CN at R.T.	3
Figure S2. Observed and theoretical mass spectra for RDAD in $[\text{M-PF}_6]^+$ mode.	4
Figure S3. Comparison of UV-Vis absorption spectra in water after in-situ oxidation using PbO_2 and the conversion of $[\text{Ru}(\text{bipy})_2\text{L}]^{2+}$ (black) to $[\text{Ru}(\text{bipy})_2\text{L}]^{3+}$ (red), where L represents the alizarin ligand.	5
Figure S4. Interconversion of different ruthenium alizarin isomers with different environments (top). RDAD in different pH solutions (bottom).	6
Figure S5. Degradation of RDAD with H_2O_2 in the aqueous buffer solution from pH 2 to pH 13. The solution was deoxygenated with N_2 before the measurement.	8
Figure S6. Concentration of RDAD versus time at 567 nm with H_2O_2 in the aqueous buffer solutions from pH 2 to pH 10.	10
Figure S7. Plot of k_1 versus pH for RDAD	11
Figure S8. HPLC of Δ - RDAD (top) and solvent blank (bottom) measured at 250 nm.	12
Figure S9. HPLC of Δ - RDAD (top) and solvent blank (bottom) measured at 567 nm.	12
Figure S10. HPLC of Λ - RDAD (top) and solvent blank (bottom) measured at 250 nm.	13
Figure S11. HPLC of Λ - RDAD (top) and solvent blank (bottom) measured at 567 nm.	13

Table S1. ¹H NMR chemical shifts (ppm) for Δ-RDAD in CD₃CN at R.T.

Complex	Fragment	H ₂	H ₃	H ₄	H ₅	H ₆	H ₇	H ₈
RDAD	alizarin	7.48 s	6.83 d	7.50 d	8.09m	7.70 t	7.52 t	7.62 d
			(7.9)	(7.8)		(7.6)	(7.6)	(8.0)
	bpy _a	8.44 d	7.89m	7.21 t	7.89m			
		(8.4)		(6.7)				
	bpy _b	8.52 d	8.09m	7.60 t	8.76 d			
		(8.1)		(6.5)	(5.6)			
	bpy _c	8.41 d	7.83m	7.18 t	7.83m			
		(8.1)		(6.8)				
	bpy _d	8.52 d	8.09m	7.50 t	8.62 d			
		(8.1)		(6.5)	(5.6)			

¹Coupling constants (*J*) are in the brackets. Unit of *J* is Hz.

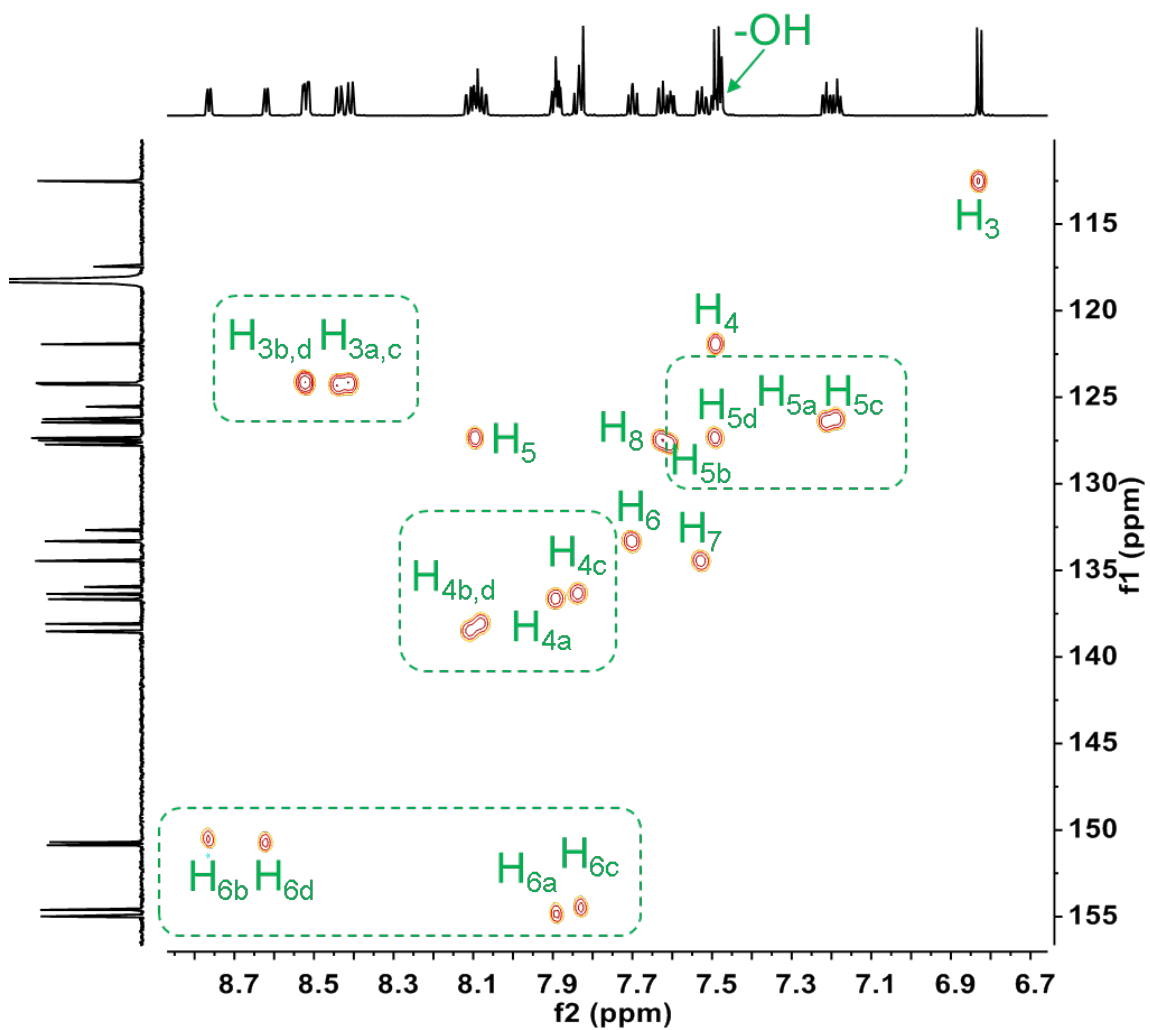


Figure S1. Labelled HSQC spectrum for Δ -RDAD in CD₃CN at R.T.

LZ_L_RU_A
(MeCN)/MeCN
C34H23N4O4RuPF6
SM: 7G

EPSRC National Facility Swansea
LTQ Orbitrap XL

NEWBEN-LZ
12/02/2018 12:38:46

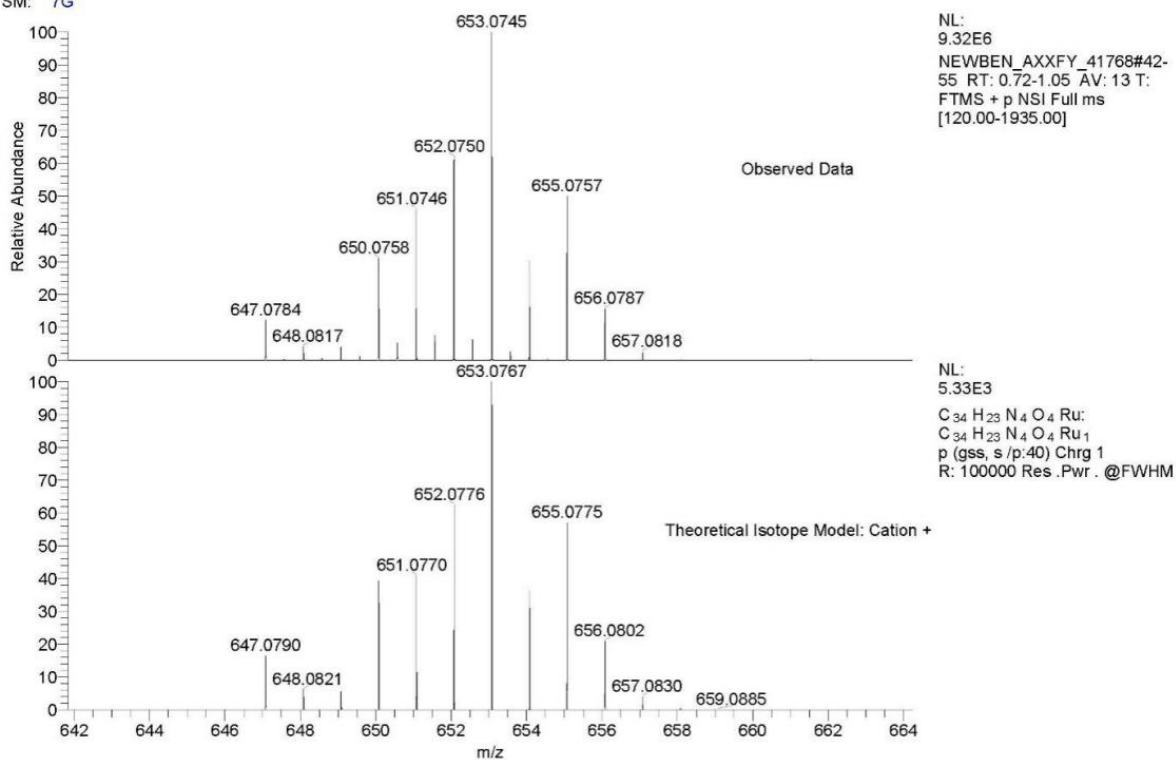


Figure S2. Observed and theoretical mass spectra for RDAD in [M-PF₆]⁺ mode.

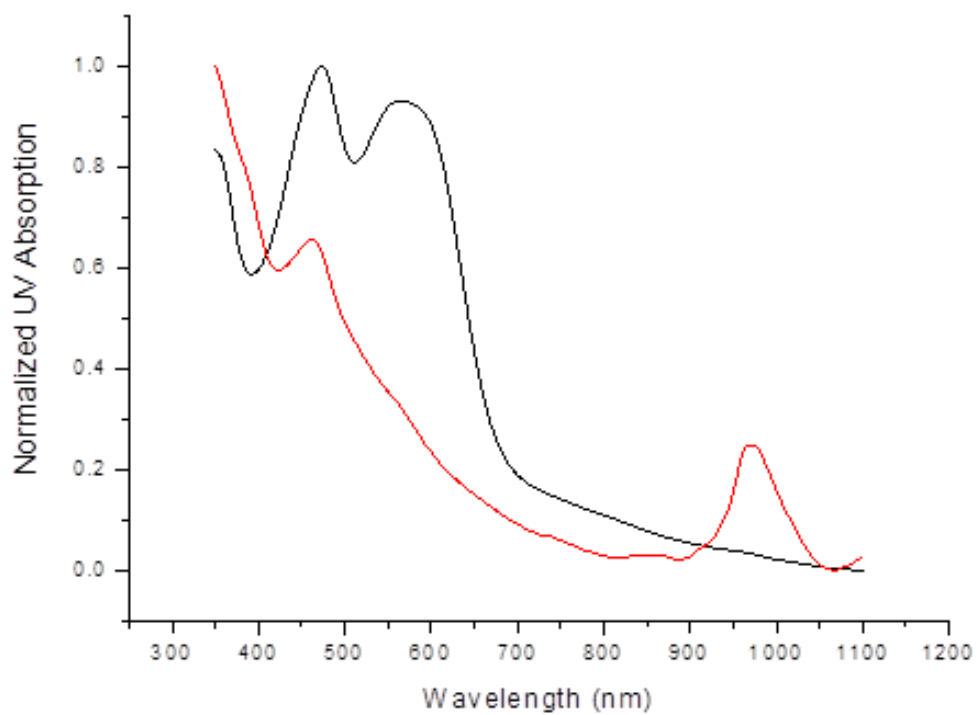


Figure S3. Comparison of UV-Vis absorption spectra in water after *in-situ* oxidation using PbO_2 and the conversion of $[\text{Ru}(\text{bipy})_2\text{L}]^{2+}$ (black) to $[\text{Ru}(\text{bipy})_2\text{L}]^{3+}$ (red), where L represents the alizarin ligand.

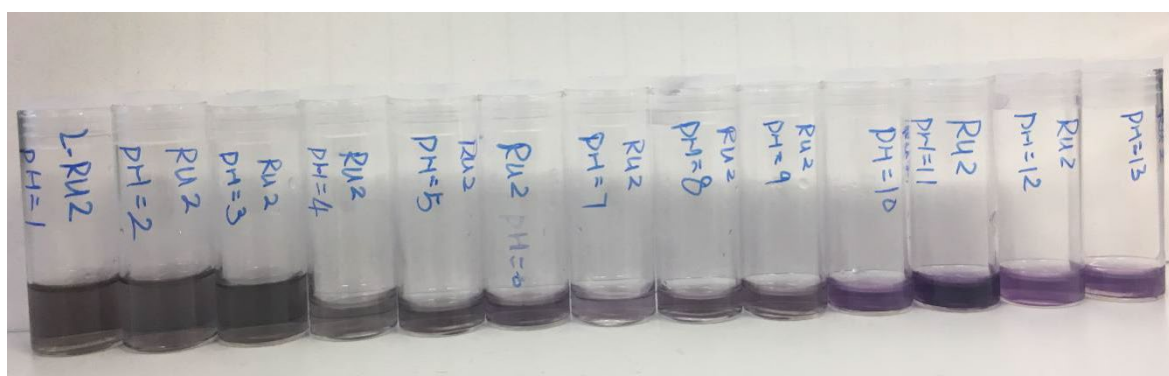
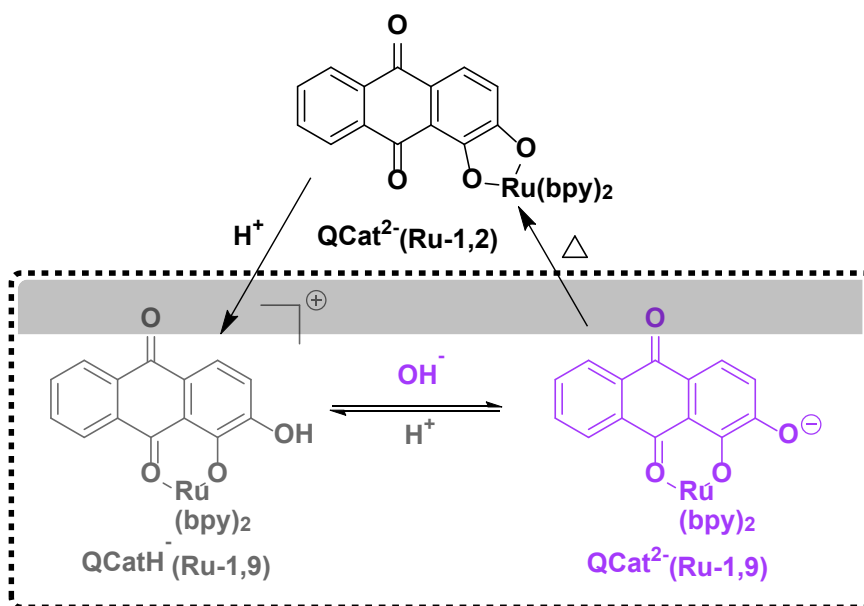
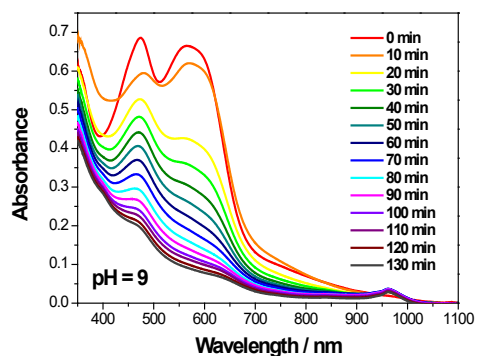
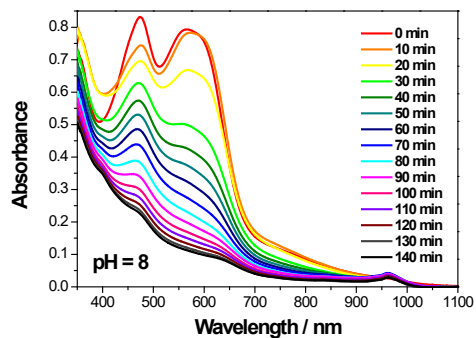
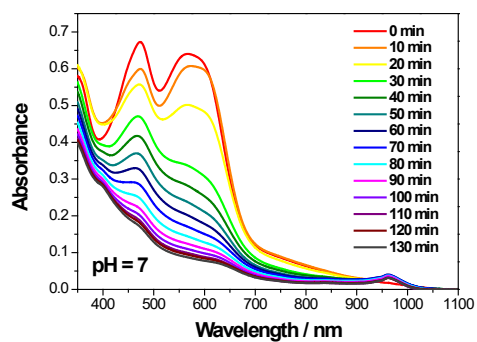
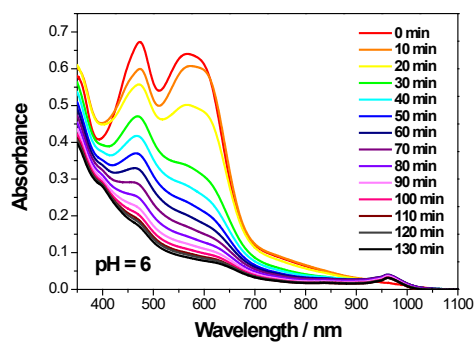
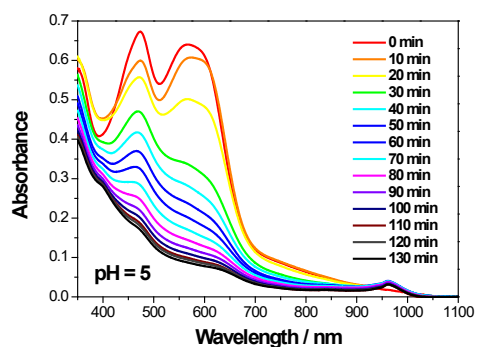
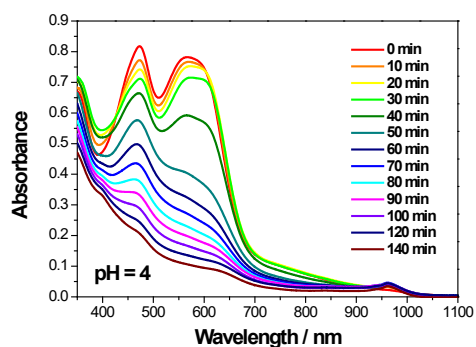
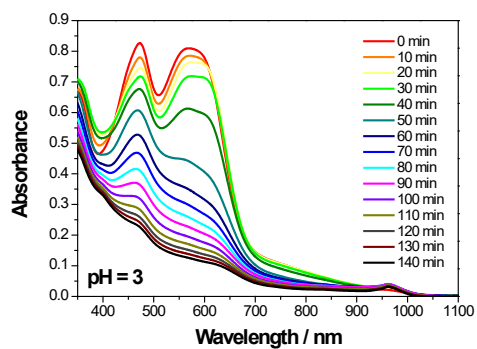
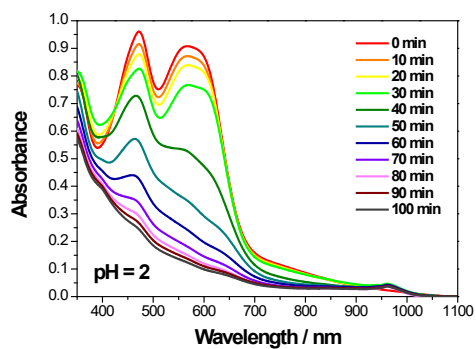


Figure S4. Interconversion of different ruthenium alizarin isomers with different environments (top). **RDAD** in different pH solutions (bottom).



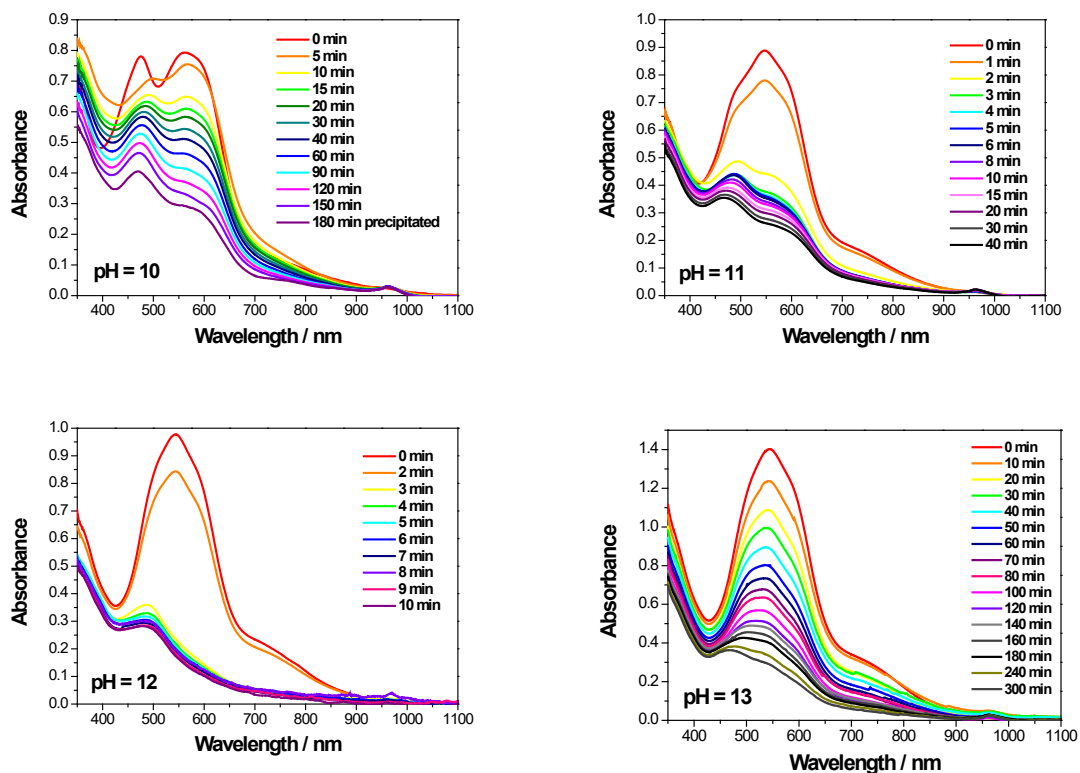
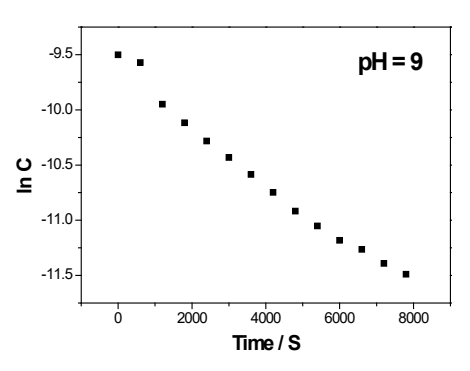
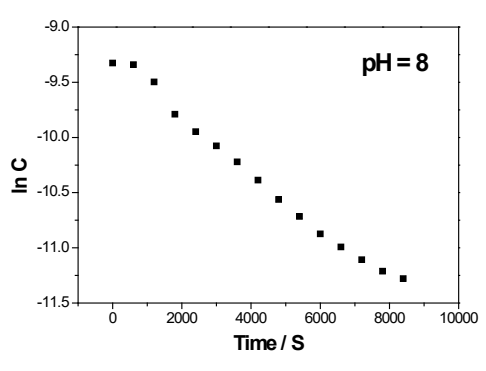
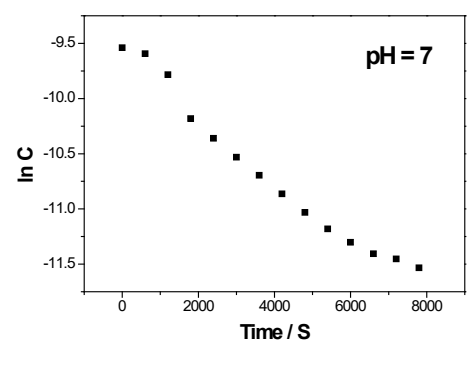
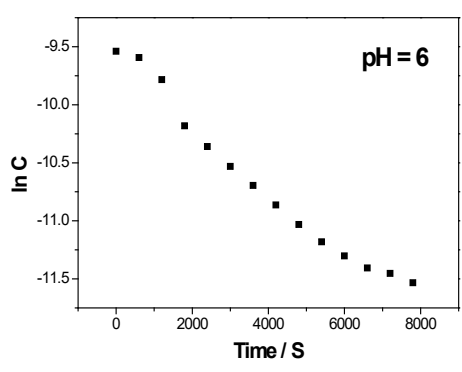
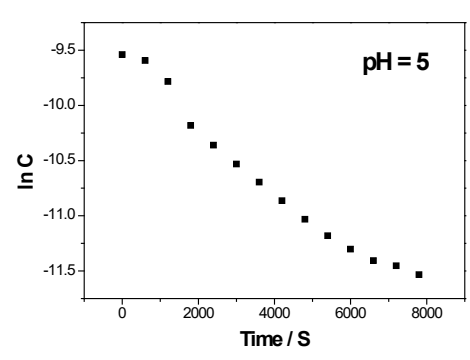
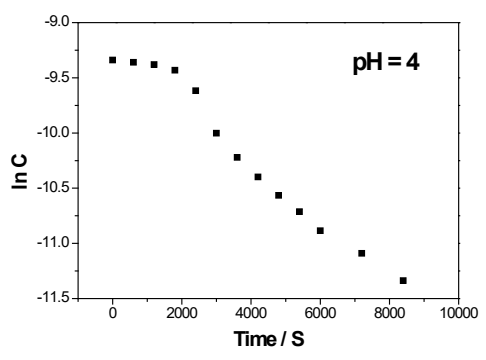
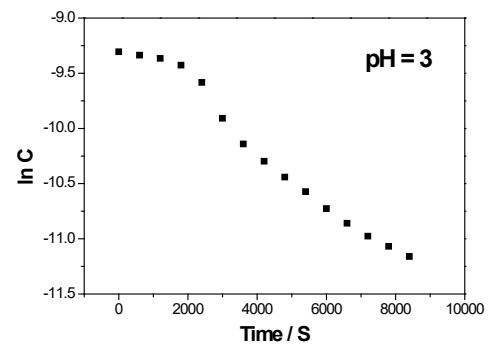
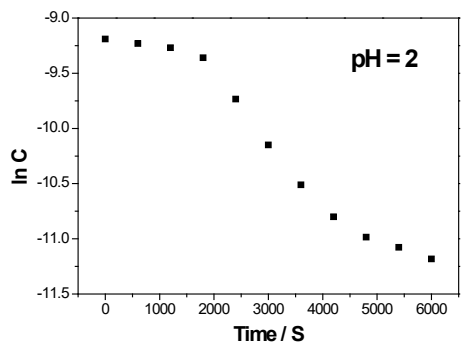


Figure S5. Degradation of **RDAD** with H_2O_2 in the aqueous buffer solution from pH 2 to pH 13. The solution was deoxygenated with N_2 before the measurement.



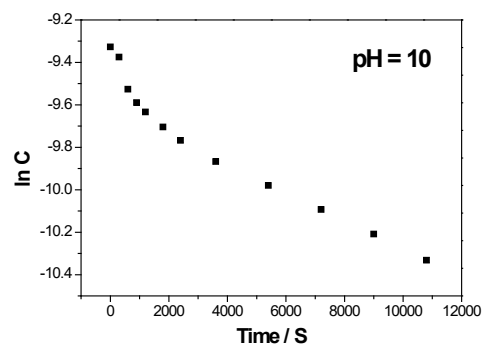


Figure S6. Concentration of **RDAD** versus time at 567 nm with H_2O_2 in the aqueous buffer solutions from pH 2 to pH 10.

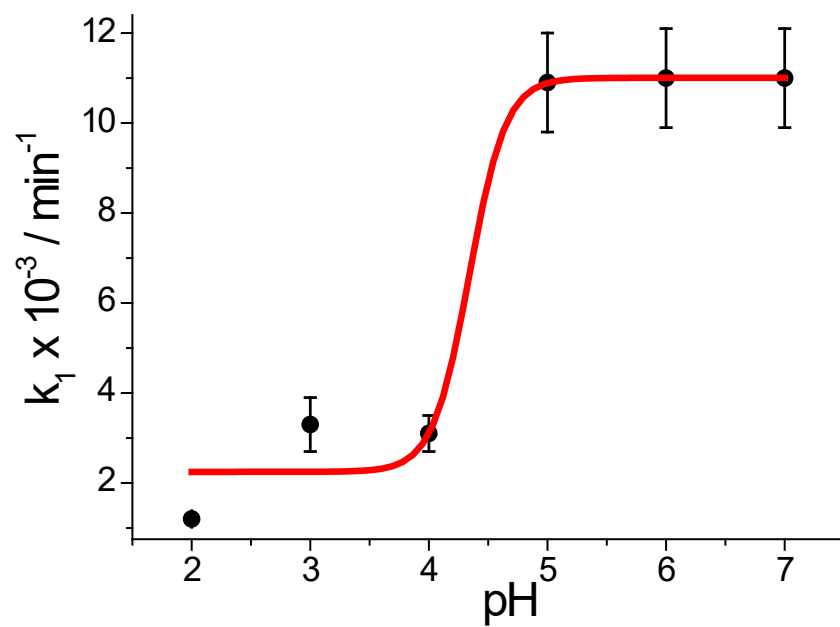


Figure S7. Plot of k_1 versus pH for **RDAD**.

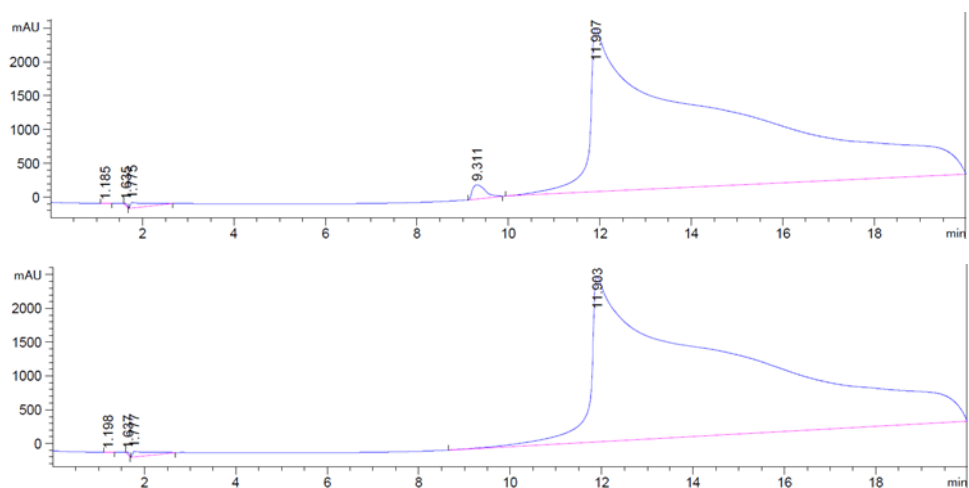


Figure S8. HPLC of Δ -RDAD (top) and solvent blank (bottom) measured at 250 nm.

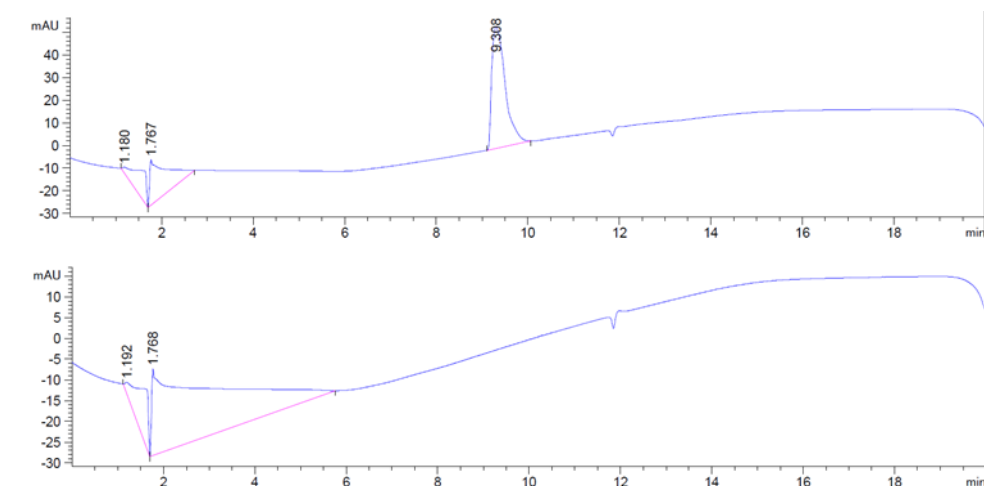


Figure S9. HPLC of Δ -RDAD (top) and solvent blank (bottom) measured at 567 nm.

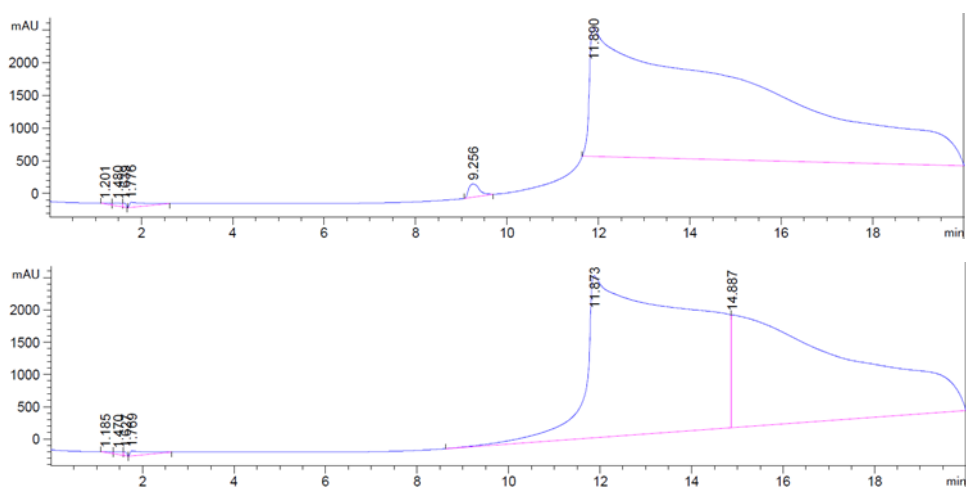


Figure S10. HPLC of Λ -RDAD (top) and solvent blank (bottom) measured at 250 nm.

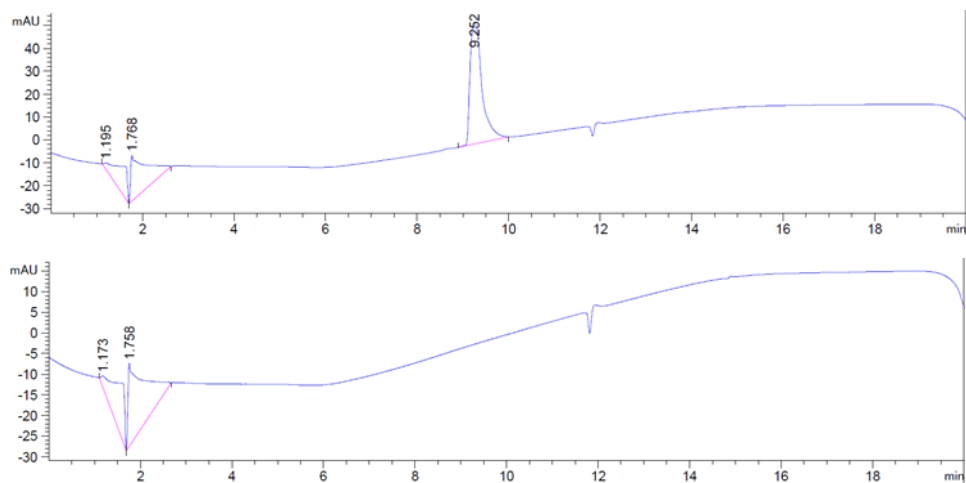


Figure S11. HPLC of Λ -RDAD (top) and solvent blank (bottom) measured at 567 nm.